nzsee
NEW ZEALAND SOCIETY FOR EARTHQUAKE ENGINEERING

Seismic response of sustainable, resilient eccentrically braced frames

M. Hasanali, K. Andisheh, N. Mago, H. Taheri, A. ShahMohammadi & M. Karpenko
NZ Heavy Engineering Research Association (NZ HERA), Auckland, New Zealand.

K. Jármai,
University of Miskolc, Miskolc, Hungary.

P. Dong
University of Michigan, Ann Arbor, USA.

G.C. Clifton
University of Auckland, Auckland, New Zealand.

G.A. MacRae
University of Canterbury, Christchurch, New Zealand.

ABSTRACT
"Circular Design" and "Construction 4.0" are two distinct concepts that can be complementary and beneficial within the construction industry in terms of minimising waste and enhancing sustainability Nascent global Construction 4.0 knowledge supports the creation of more resilient infrastructure through integrating and utilising digital technologies and advanced automation in the construction industry to optimise resource management, improve energy efficiency and enhance sustainability throughout the construction lifecycle. However, Circular Design focuses on sustainability beyond the construction phase into the entire lifecycle of a resilient building, emphasising reducing waste, reusing materials, and minimising environmental impact. Demountability/reuse of steel structures rather than landfilling or recycling them can be considered endeavours that are aligned with both Circular Design and Construction 4.0 concepts to develop a sustainable, resilient structural system with low carbon emissions. This study aims to develop an optimised design of Reusable Eccentrically Braced Frames (R-EBF) as one of the lateral force-resisting systems in New Zealand steel structures to enable easy disassembly at the end of their lifecycle or during operational time. Initially, an evaluation is conducted to compare the seismic performance and environmental impacts of the innovative R-EBFs with those of the current EBF systems. Then, the optimisation is performed to minimise the weight of an innovative R-EBF, resulting in the project cost's reduction. Consequently, this work contributes to the reduction of the environmental impacts of the built environment by minimising material production and associated carbon emissions, resulting from both minimising the mass of the structure and the reusability of some of the resilient structural components.

1 INTRODUCTION

Eccentrically Braced Frames (EBF) have been widely employed as dependable structural systems for effectively withstanding lateral seismic forces, incorporating the concept of ductile design to reduce the level of design seismic loads. The main concept in designing an EBF is to amalgamate the benefits of both a Moment Resisting Frame (MRF) and a Concentrically Braced Frame (CBF) as lateral load-resisting systems within a unified structural framework (Kazemzadeh Azad and Topkaya, 2017). Therefore, the EBFs can be regarded as hybrid structural systems, combining much of the elastic stiffness of CBFs with the ductility and energy dissipation capacity inherent in MRFs (Engelhardt and Popov, 1989). The strength, stiffness, and ductility of the active links, which serve as the yielding elements in the seismic resisting system and which connect the braces within the frame to other structural components like columns and collector beams, significantly affect the design of an EBF (Mansour et al., 2011). Generally, the active link segments are deigned to yield unlike the other members of an EBF system designed to maintain the essentially elastic behaviour. In the initial EBFs, the active link is interlinked to the collector beams while in more modern EBFs, a bolted replaceable active link is employed to facilitate the replacement of damaged active links and to allow a different member size for the active link than is needed for the collector beam. Figure 1 demonstrates two typical configurations of EBF systems, featuring different structural components in each design.

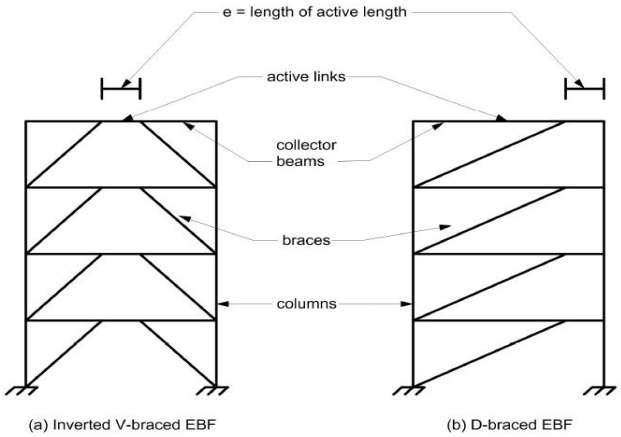

Figure 1: Two common EBF configurations (HERA report P4001, 2013).

In traditional EBFs, the design of collector beams entails a challenging balance in which these members need to yield in the link region while concurrently resisting forces resulting from strain hardening in the surrounding areas of the link. This equilibrium necessitates an iterative process, often leading to the use of larger-than-optimal link elements. Consequently, this may impose higher demands on other components of the EBF system, resulting in structures that are conservatively designed and increased overall costs (HERA report P4001, 2013). In contrast, EBFs with bolted replaceable active links effectively address this drawback by enabling independent control over beam stiffness and required strength.

In recent decades, several research efforts have been dedicated to evaluate the seismic behaviour of both traditional EBFs (Engelhardt and Popov, 1989; Ghobarah and Ramadan, 1994; Kasai and Popov, 1986a, 1986b; McDaniel et al., 2003; Okazaki and Engelhardt, 2007; Popov et al., 1987) and EBFs featuring replaceable active links (Dubina et al., 2008; HERA report P4001, 2013; Mansour et al., 2011; Stratan and Dubina, 2004). It should be also noted that the performance of EBF buildings during the 2010/2011 Christchurch earthquakes aligned with expectations, demonstrating the effectiveness of the current capacity design procedure (Clifton et al., 2011).

This study aims to propose a novel low-damage Reusable EBF (R-EBF) system featuring bolted connections that is aligned with the CE concept to develop a sustainable structural system with reduced carbon emissions. The concept of low damage design is used in this system to enhance its resilience. The goal is to ensure that this reusable system remains functional and can be quickly used at the end of the building's lifecycle in another structure, contributing to the overall safety and sustainability of the built environment. Subsequently, an optimisation procedure is conducted to minimise the weight of an innovative R-EBF, leading to the project cost's reduction.

2 DEVELOPMENT OF CASE STUDIES

In the present study, the ground level of an eight-storey EBF, as previously assessed in the HERA P4001 technical report, is selected as a case study (see Figure 2). In this frame, the floor system, characterised by a secondary beam spacing of 9 m, runs parallel to the EBF, with perpendicular beams supported by the columns. In cases where the secondary beams find support from the collector beam, it is important to consider these additional loads in the EBF's design. Moreover, it is essential to ensure that the placement of secondary beams avoids reliance on the active link for support.

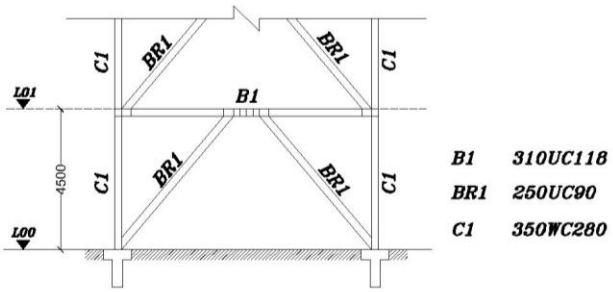

Figure 2: EBF elevation at ground level (HERA report P4001, 2013).

2.1 EBF systems

Five distinct EBF systems are examined in this study, comprising the traditional EBF (T-EBF), the non-reusable EBF with replaceable active link (i.e., existing EBF, E-EBF), three innovative reusable EBFs (R-EBF) with different combinations of stiffeners. While all connections except those for the shear links are welded connections in the design of T-EBF and E-EBF, the reusable EBFs are designed for disassembly by replacing all welded connections with bolted connections. Different combinations of stiffeners have been applied to the R-EBFs to investigate the capability of energy dissipation of each system. While in one of the R-EBFs, the stiffeners are incorporated into the bolted connections of the braces as well as the vertical stiffeners in the web of the active link (R-EBF-1), in another case studies, the stiffeners in the bolted connections of the braces are omitted (R-EBF-2), and in a different scenario, the web vertical stiffeners are removed (R-EBF-3). The rationale behind eliminating intermediate web stiffeners is based on findings from the study conducted by Volynkin et al. (2019). According to their research, elements with a web slenderness lower than 25 (i.e., $d_1/t_w \leq 25$) do not require intermediate stiffeners as they are not susceptible to buckling. Notably, in this study, the web slenderness of the shear link is identified as 23. Figure 3 demonstrates the active link of these frames, highlighting their variations.

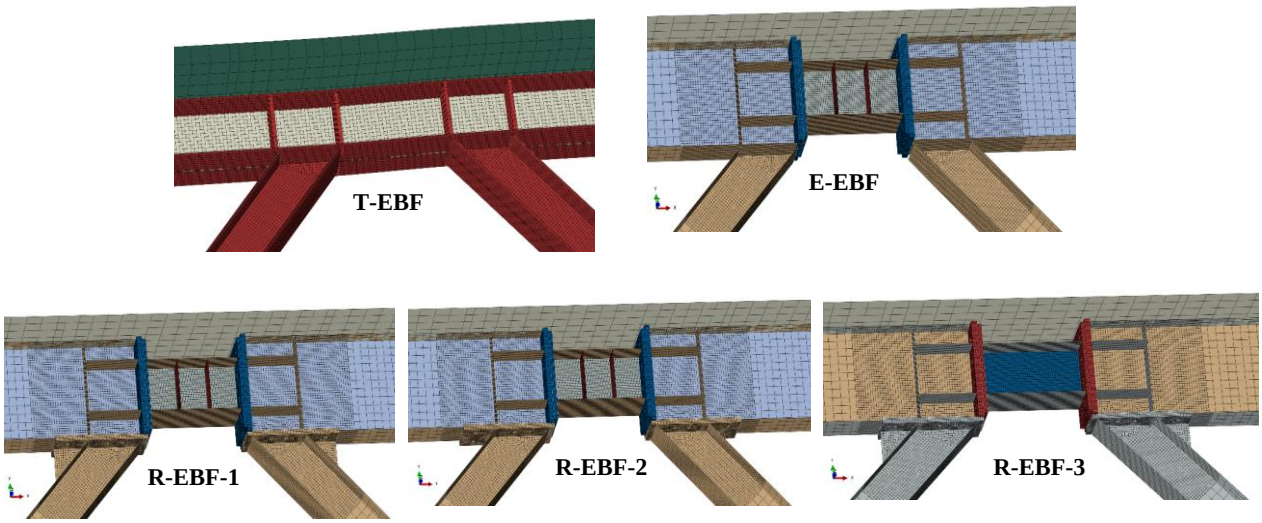

Figure 3: Details of shear link connections for different investigated EBFs.

2.2 EBF connections

In this section, the details of the connections of E-EBF and studied R-EBFs are compared. Figure 4 illustrates the connection details for the E- EBF. In Figure 4 (a), while the connection between the brace and the column to the foundation is displayed, Figure 4 (b) demonstrates a bolted connection between the collector beam and the column, where the brace is welded to the collector beam. Figure 4 (c) shows both the welded connection between the brace and the collector beam and the bolted connection between the collector beam and the replaceable shear link in the E-EBF system. These connections for the E-EBF align with New Zealand engineering best practices and have been designed in accordance with the HERA P4001 technical report (2013). The comprehensive information regarding the T-EBF connections is available in the HERA P4001 technical report (2013). Due to space constraints, these specifics are not presented in the current paper.

Figure 5 provides an illustration of the connection specifics for the reusable EBFs (R-EBF) featuring a replaceable shear link and stiffeners. The key distinction in the connections of different R-EBF systems is integrating different combination of stiffeners in each system as outlined in Section 2.1.

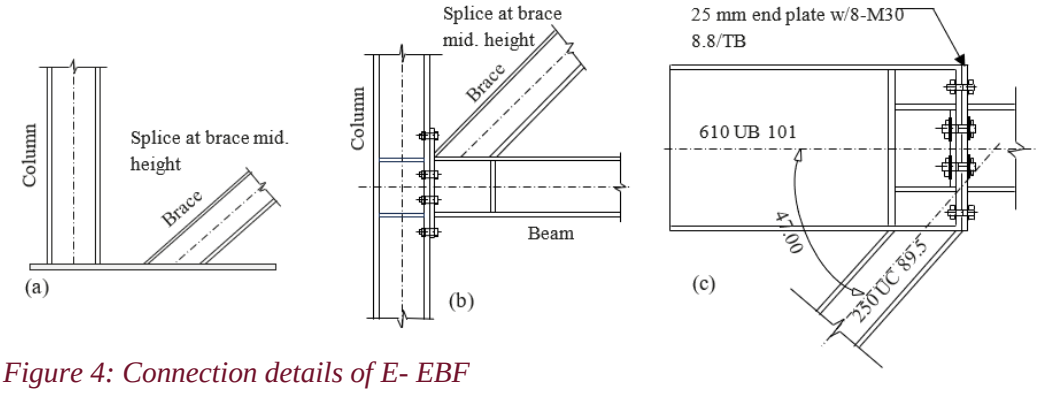

Figure 4: Connection details of E- EBF

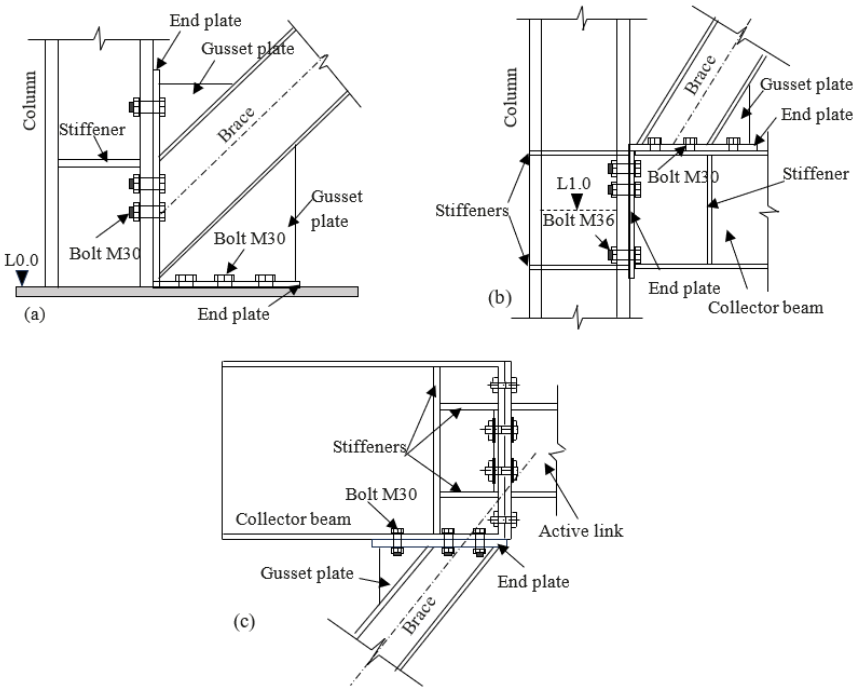

Figure 5: Connection details for reusable EBFs.

3 COMPARING THE SEISMIC PERFORMANCE OF INVESTIGATED EBFS

The simulation was conducted in two dynamic implicit quasi-static steps. Step Time 1 represents the tightening of all M30 bolts, which marks the initiation of cyclic displacement, indicating that a bolt force of 335 kN equivalent to a bolt length adjustment of 0.321 mm is in place. In Step-2, cyclic enforced displacements have been applied on the left and right collector beam to column connections at both floor levels. The duration of Step-2 is 74, with each unit of time representing one peak displacement.

The simulation results for the rigid frames, namely traditional with continuous collector beam (T-EBF) and existing with replaceable shear link (E-EBF) show the high stress region and developed equivalent plastic strain (PEEQ), which is a scalar variable that is used to represent the material's inelastic deformation, at the active link. However, T-EBF has a significant capacity compared to the other studied systems. In contrast, high stress region and PEEQ are further developed at the collector beam web and bottom flange junction where the brace is bolted (see Figure 6). Further analyses are required for detailed assessment of the whole structure.

The von Mises stress contribution from the five options also shows higher stress at the collector beam web and bottom flange junction where the brace is bolted in the R-EBFs compared to the T-EBF and E-EBF in which the high stress region is concentrated at the active link (see Figure 7).

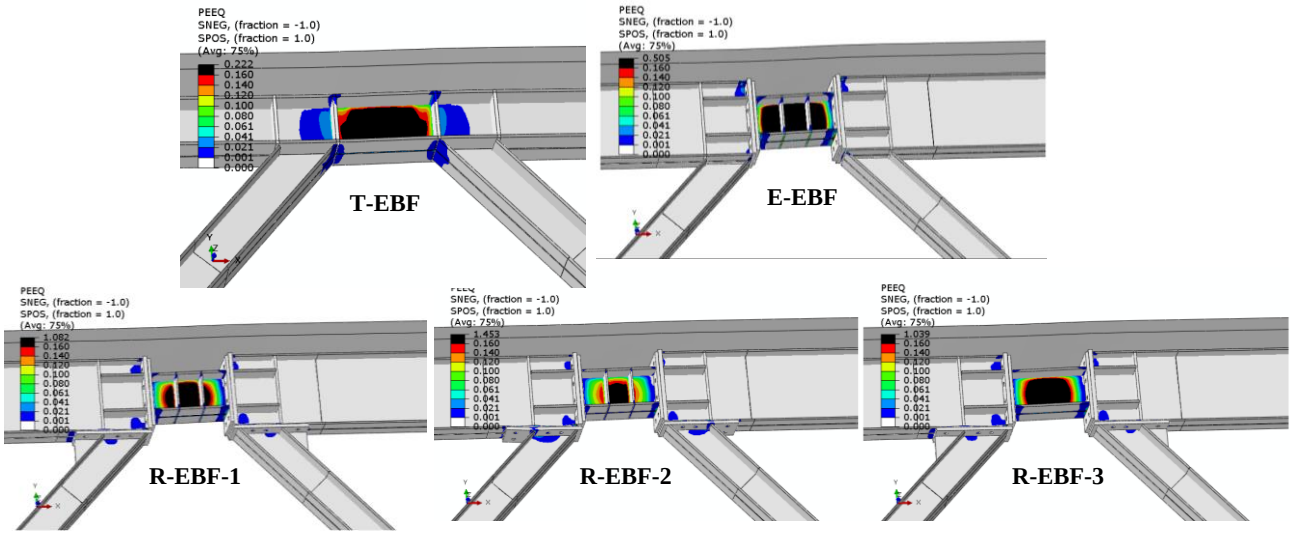

Figure 6: Equivalent plastic strains (PEEQ) in the active links of three investigated EBFs.

Figure 8 demonstrates the hysteresis force-displacement responses of five studied EBFs. As can be seen, the dissipated energy of the T-EBF is significantly higher than that in the other frames featuring replaceable (E-EBF) and R-EBF systems (R-EBF-1 and R-EBF-2), which is consistent with the results showing high developed PEEQ and stress in the active links of this system. It is also important to note that the hysteresis curves of R-EBF-2 and R-EBF-3 systems are almost identical. This aligns with the findings presented in the literature by Volynkin et al. (2019), indicating that the intermediate stiffeners for elements with low web slenderness ratios (i.e., $d_1/t_w \leq 25$) can be eliminated as these elements do not undergo buckling. These hysteresis curves will be further used in Sections 3.1 and 3.2 to evaluate cyclic performance and to quantify the dissipated energy of each system, respectively, to demonstrate the capacity of each system to withstand the seismic loads.

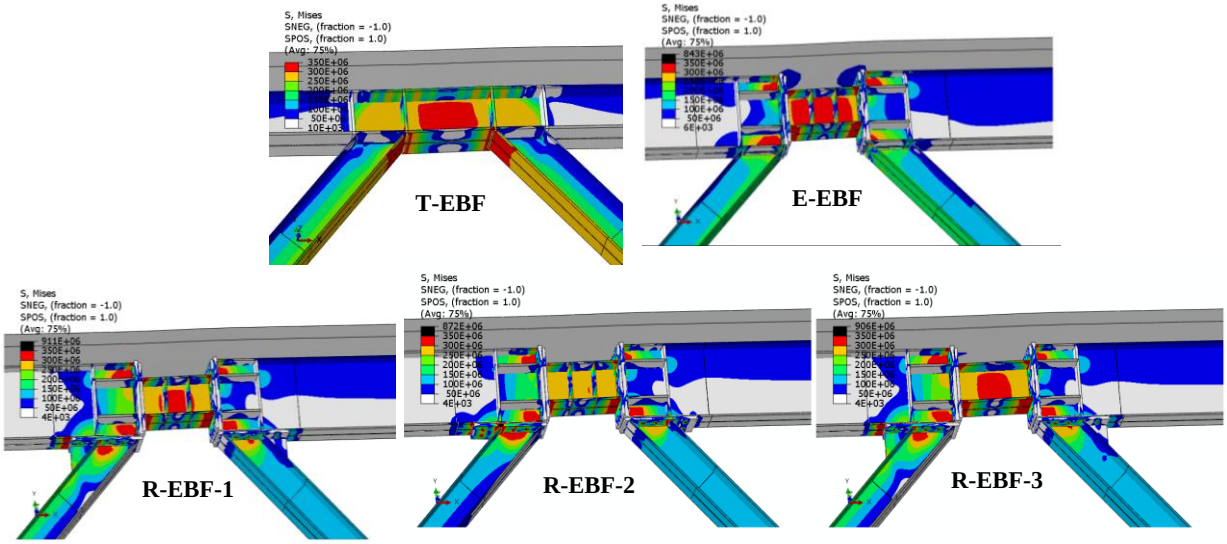

Figure 7: Von Mises stresses of three studied EBF systems.

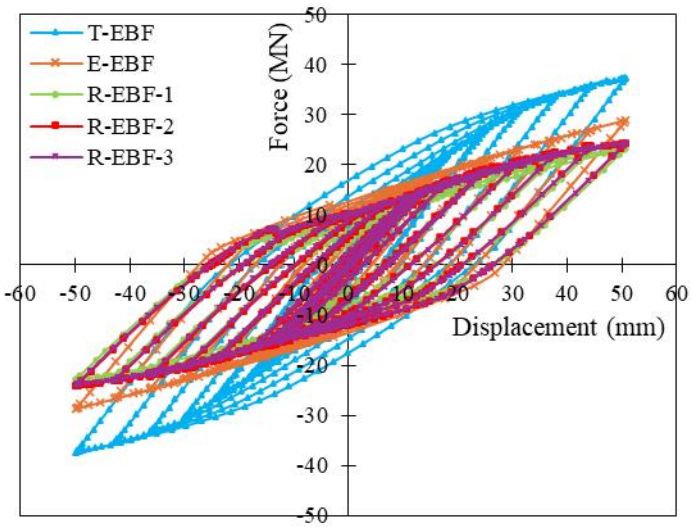

Figure 8: Hysteresis force-displacement responses of three studied EBFs.

3.1 Cyclic behaviour

The key characteristics of the cyclic behaviour of the studied EBFs based on the hysteresis responses are presented in Table 1. In this table, F_y denotes the yield load; Δ_y represents the yield drift value; Δ_u signifies the ultimate drift; $K_{elastic}$ defines as the initial modulus; F_{max} stands for maximum applied load; $\mu = \Delta_u/\Delta_y$ indicates the drift ductility; $\Delta_p = \Delta_u - \Delta_y$ denotes the plastic drift. It is noteworthy that, although the cyclic performance of the T-EBF considerably surpasses that of E-EBF and R-EBFs, there is not a substantial difference between the performances of E-EBF and R-EBFs. The results show the maximum load resisted by R-EBF-1 (i.e., with stiffener) is over 16% less than that for E-EBF. The ductility achieved for R-EBF-1 was 85% of that for E-EBF. Reusability also resulted in at least 15% reduction in the elastic stiffness of EBF. It is important to note the ductility of the R-EBF-3 is similar to the that of the T-EBF.

Table 1: Characteristics of the cyclic behaviour of the studies EBFs.

Specimen	F_y (kN)	Δ_y (%)	$K_{elastic}$ (MPa)	F_{max} (kN)	Δ_u (%)	μ	Δ_p(%)
T-EBF	2600	0.170	1423	3728	0.6	3.52	0.43
E-EBF	1550	0.150	1033	2870	0.6	4.00	0.45
R-EBF-1	1500	0.175	857	2430	0.6	3.42	0.43
R-EBF-2	1475	0.178	831	2300	0.6	3.38	0.42
R-EBF-3	1474	0.168	835	2430	0.6	3.57	0.43

3.2 Dissipated energy

Dissipated energy refers to the amount of energy that is absorbed and dissipated by the structure during seismic loading cycles. In this section, a comparative analysis is carried out to quantify the dissipated energy by each studied EBF system.

Table 2 lists the dissipated energy values for five studied EBF systems (i.e., T-EBF, E-EBF, R-EBF-1 to R-EBF-3) at different levels of applied displacement. The computation of dissipated energies is based on the area enclosed by the hysteresis force-displacement curve, as illustrated in Figure 8, for each of the examined EBF

systems. To facilitate a straightforward comparison, the dissipated energy of each system is normalised with respect to the corresponding dissipated energy of the traditional EBF (T-EBF) at a particular drift ratio. From Table 2, it can be revealed that the normalised dissipated energy of E-EBF in the small drift ratio is higher than that in the T-EBF, attributing to a more uniform distribution of forces within the T-EBF, preventing localised concentration of stress. This uniform distribution can help to mitigate deformation and energy dissipation in the early stages of drift. While for the higher drift ratio, there is a reduction of about 30% in the energy distribution of the E-EBF compared to the T-EBF. The normalised dissipated energy of R-EBF-1 falls within the range of 0.92 to 0.69, which subsequently reduces to a range of 0.88 to 0.62 for the R-EBF-2 system. Furthermore, R-EBF-3 has the maximum energy dissipation capacity among the three studied R-EBFs, attributed to the fact that incorporating the intermediate web stiffeners reduces the deformation capacity of the active link, resulting in the lower energy dissipation capacity, confirming the results of the study conducted by Volynkin et al. (2019). Although the results show that the R-EBFs have less energy dissipation compared to T-EBF and E-EBF, they meet the seismic performance requirements for structures exposed to moderate to severe earthquakes. Further studies can enhance the seismic performance of R-EBFs, thereby contributing to a more significant reduction in environmental impact.

Table 2. Dissipated energy of different studied EBFs based on various drift percentages.

Displacement (mm)	**Drift** (%)	**Dissipated Energy** ($kN.m$)					**Normalised dissipated energy**				
		T-EBF	E-EBF	R-EBF-1	R-EBF-2	R-EBF-3	T-EBF	E-EBF	R-EBF-1	R-EBF-2	R-EBF-3
25	0.31	39.5	52.9	36.5	32.8	38.2	1.00	1.34	0.92	0.83	0.97
31	0.39	65.8	83.7	62.2	58.1	65.8	1.00	1.27	0.95	0.88	1.00
37	0.46	107.4	123.9	92.9	85.7	92.9	1.00	1.15	0.86	0.80	0.86
45	0.56	165.8	154.8	125.5	117.8	126.0	1.00	0.93	0.76	0.71	0.76
50	0.63	234.5	196.7	161.3	145.4	161.9	1.00	0.84	0.69	0.62	0.69

4 CIRCULAR ECONOMY AND ENVIRONMENTAL IMPACTS OF EBFS

A comprehensive definition of a CE underscores its inherent focus on restoration and regeneration (Mulhall et al., 2019). In recent years, there has been a growing emphasis on the CE, prompted by factors such as population growth, increasing infrastructure demands, climate change, and the potential for resource scarcity (Cruz Rios et al., 2021). The central aim of the CE revolves around the promotion of reuse, aiming to alleviate environmental impacts not only during the production phase but also throughout the post-consumer lifecycle of a product (Dimitropoulos et al., 2021). The evolution of circular structural systems is contingent upon the application of Circular Design principles, integrating CE concepts into the construction industry. This integration is a critical aspect of Construction 4.0, enabling the use of reusable, optimised, and resilient structural systems to reduce waste, conserve resources, and advance sustainability.

The embodied carbon of the frames was compared to assess the environmental impact of the EBFs. The analysis's system boundary encompasses production modules (A1-A3), end-of-life modules (C3-C4), and post-life module (D). The emission factors for Global Warming Potential (GWP) were obtained from the Environmental Product Declaration (EPD) of Hot Rolled Structural Steel (Registration Number: S-P-01547 Version 1.2). Table 3 presents emission factors. For Scenario 1 (steel recycling at the end-of-life) the emission factors are as per the EPD. However, in scenario where steel is reused, module D of the EPD has been updated to reflect the environmental benefits of steel reuse beyond its initial life cycle. Consequently, in the steel reuse

scenario, the values for the production phases (A1-A3) are negated and replaced with the recycling value. While this approach may slightly deviate from the actual numbers for steel reuse due to data limitations, it is considered a closely accurate assumption. Detailed information can be found in a recent study conducted by Andisheh et al. (Andisheh et al., 2024).

In this evaluation, two different scenarios have been taken into account. In the first scenario, steel is employed in an existing building that, upon reaching the end of its life, will undergo demolition, and the materials will be directed to recycling. Subsequently, a new building will be erected using new steel. The second scenario highlights the advantages of reusability. In this case, the steel frame is integrated into a building explicitly designed for disassembly, ensuring its potential repurposing in another structure after completing its life cycle. Table 4 presents the emissions associated with each scenario across individual modules and overall. The findings indicated that frames designed for reuse, when reused after their initial life, can affectively lead to significant reduction in the cradle-to-cradle embodied emissions of steel compared to frames reconstructed from new steel.

Table 3: Total Emissions Factors for Building Scenarios.

$Kg\ CO_2\ Eq$ per tonne of steel	Today		
	A1-A3	C	D
Scenario 1: Steel Recycling at the end-of-life	3320	7	-2100
Scenario 2: Steel Reuse at the end-of-life	3320	7	-3320

Table 4. Embodied carbon emissions comparison for the studied frames.

Frame type	Frame Weight ($Tonne$)	A1-A3 (Kg CO_2 Eq)	C3-C4 (Kg CO_2 Eq)	D (Kg CO_2 Eq)	Overall (Kg CO_2 Eq)
T-EBF	4.859	16131.9	34.0	-10203.9	5962.0
E-EBF	4.717	15660.4	33.0	-9905.7	5787.8
R-EBF-1	4.752	15776.6	33.3	-15776.6	33.3
R-EBF-2	4.73	15703.6	33.1	-15703.6	33.1
R-EBF-3	4.726	15690.3	33.1	-15690.3	33.1

5 OPTIMISATION OF THE EBF SYSTEM

Using mathematical optimisation techniques, can minimise the mass, cost, or environmental effects of the structure, while all constraints related to stress, deformation, stability, manufacturability, etc., are considered (Farkas and Jármai, 2013). When optimising steel structures, regardless of whether the objective is to reduce either weight or cost, the result is a reduction in the mass (weight) of the utilised steel. Since the environmental impact is closely correlated with the structure's mass, the weight reduction has a direct bearing on the reduction in environmental impact. After evaluating the performance of the innovative reusable EBF systems (R-EBF-1 & 3) compared to the T-EBF and E-EBF, the other objective is to develop a practical methodology for enabling the development of optimised R-EBF systems to minimise environmental impact to the greatest extent possible. This project is currently in progress and the optimisation process will cover the entire R-EBF system including shear links, braces, beams, and columns as well as connections. This section presents specific results, focusing on the optimisation of shear active links of the eight-storey EBF system specified in Section 2. For the optimisation process, the Generalised Reduced Gradient (GRG) (Lasdon et al., 1973) algorithm, which is one of the most popular methods to solve nonlinear optimisation, was used. To ensure that the proposed cross-

sections in the optimisation process align with the scope of design standards (HERA report P4001, 2013; NZS 3404 Part 1&2, 1997), the following constraints are considered:

The shear link length needs to satisfy the following criteria:

$$\boldsymbol{d < e_{link} \leq 1.6 \frac{M_{sx}}{V_w}} \quad (1)$$

The other constraints are the shear and bending demand limitations as well as the inelastic rotational angle between the active link and the adjacent beam, as follows:

$$\boldsymbol{V^*_{link} \leq \emptyset V_w} \quad (2)$$

$$M^*_e \leq 0.75 \emptyset M_{sx} \quad (3)$$

$$\gamma_p \leq 0.08, \gamma_p = \frac{L}{e}\theta_p, \text{where } \theta_p = tan^{-1}\left(\frac{(\mu-1)k_d \Delta_g}{H}\right) \quad (4)$$

In the above equations, d denotes the cross-sectional web height; e_{link} defines as the shear link length; M_{sx} and V_w are the bending and shear capacities; respectively. The variables V^*_{link} and M^*_e refer to the shear and bending demands in the active link, respectively. The factors Δ_g, H, L and e refers to the displacement of the top level, the total building height, the beam span and the active shear link length, respectively.

The objective function is to minimise the mass of the shear link (M) in each storey:

$$\boldsymbol{M_{optimised} \leq M_{original}} \quad (5)$$

Table 5: Optimisation results for active shear links

Level	Original shear link sections	Optimised shear link sections	e_{link} (mm)	$\emptyset V_w$ (kN)	V^*_{link} (kN)	$\emptyset M_{sx}$ $(kN.m)$	M^*_e $(kN.m)$	$1.6\frac{M_{sx}}{V_w}$ (mm)
L08	200UC52.2	150UC30	600	158.5	108.6	64.2	32.6	648.2
L07	200UC52.2	200UC46.2	600	228.3	176.7	121.8	53.0	853.3
L06	200UC52.2	200UC52.2	600	250.2	235.4	138.2	70.6	884.0
L05	250UC89.5	200UC59.5	600	306.5	284.8	157.7	85.4	823.1
L04	250UC89.5	250UC72.9	600	334.4	324.9	242.2	97.5	1158.9
L03	250UC89.5	250UC89.5	600	408.2	355.6	277.2	106.7	1086.4
L02	310UC118	250UC89.5	600	408.2	376.9	277.2	113.1	1086.4
L01	310UC118	310UC118	600	534.0	500.1	443.5	150.0	1328.9

Comparing the mass of the original shear links with the optimised components revealed a notable 16% decrease, leading to a more substantial reduction in environmental impact (see Table 5). While this optimisation specifically targeted a segment of the system, ongoing efforts are directed into the comprehensive optimisation of the entire R-EBF system, potentially minimising costs and environmental impacts. To facilitate widespread applicability, a practical optimisation methodology will be presented, offering a systematic approach applicable to enhancing the efficiency of any R-EBF system. The proposed design methodology aims to contribute to a more sustainable built environment. It is important to mote, after developing the optimised system, a thorough seismic performance assessment will be conducted to ensure its safety.

6 CONCLUSIONS

Circular Design, an essential philosophy in the construction sector emphasising CE principles, plays an important role in Construction 4.0. It incorporates the use of flexible, adaptable, and resilient structures and infrastructure designs to minimise waste, conserve resources, and foster sustainability. The significance of reusing steel is highlighted as a key factor in attaining CE goals and striving for a net-zero carbon footprint. This research concentrates on advancing the concept of reusable structural system design specifically tailored for seismic frame design, a common feature in steel-frame structures found in New Zealand.

The objective of this research was to develop the design of a R-EBF system, serving as a lateral force-resisting system within steel structures in New Zealand. The aim was to facilitate easy disassembly either at the end of their lifecycle or during operational time. The initial phase involved evaluating the seismic performance and environmental effects of the novel R-EBFs, comparing them with the existing EBF systems. Subsequently, optimisation techniques were used to minimise the weight of the innovative R-EBF, ultimately leading to a reduction in project costs.

For five studied EBFs, the cyclic force-displacement responses have been investigated and it was demonstrated that although the cyclic performance of E-EBF is better than that of R-EBFs, there isn't a significant difference in their performances. Furthermore, a comparative analysis was conducted to quantify the dissipated energy by each studied EBF system. While the numerical results demonstrated that reusable EBFs meet the seismic performance requirements for structures exposed to moderate to severe earthquakes, further research is necessary to improve their seismic performance. Furthermore, the assessment of the environmental effects of the examined EBF systems was conducted based on the embodied carbon of each system. The findings demonstrated that the implementation of innovation R-EBFs could significantly decrease the embodied emissions of steel. Lastly, the optimisation of the active shear links led to the 16% reduction in the mass of shear links compare to the original elements.

7 ACKNOWLEDGEMENT

The research was enabled by Endeavour funding from the New Zealand Ministry of Business, Innovation and Employment (MBIE) awarded to HERA for the project titled “Developing a Construction 4.0 transformation of Aotearoa New Zealand's construction sector.

8 REFERENC

Andisheh, K., Jármai, K., Taheri, H., Nandor, M., Maryam, H., 2024. EVALUATING SEISMIC RESPONSE OF INNOVATIVE REUSABLE ECCENTRIC BRACED FRAMES (EBF). Presented at the 18th World Conference Earthquake Engineering (WCEE 2024).

Clifton, C., Bruneau, M., MacRae, G., Leon, R., Fussell, A., 2011. Steel structures damage from the Christchurch earthquake series of 2010 and 2011. Bull. N. Z. Soc. Earthq. Eng. 44, 297–318.

Cruz Rios, F., Grau, D., Bilec, M., 2021. Barriers and Enablers to Circular Building Design in the US: An Empirical Study. J. Constr. Eng. Manag. 147, 04021117. https://doi.org/10.1061/(ASCE)CO.1943-7862.0002109

Dimitropoulos, A., Tijm, J., in’t Veld, D., 2021. Extended Producer Responsibility: Design, Functioning and Effects. Neth. Environ. Assess. Agency CPB Neth. Bur. Econ. Policy Anal.

Dubina, D., Stratan, A., Dinu, F., 2008. Dual high-strength steel eccentrically braced frames with removable links. Earthq. Eng. Struct. Dyn. 37, 1703–1720. https://doi.org/10.1002/eqe.828

Engelhardt, M.D., Popov, E.P., 1989. On design of eccentrically braced frames. Earthq. Spectra 5, 495–511.

Farkas, J., Jármai, K., 2013. Optimum Design of Steel Structures. Springer Berlin Heidelberg, Berlin, Heidelberg. https://doi.org/10.1007/978-3-642-36868-4

Ghobarah, A., Ramadan, T., 1994. Bolted link-column joints in eccentrically braced frames. Eng. Struct. 16, 33–41.
HERA report P4001, 2013. Seismic design of eccentrically braced frames. New Zealand Heavy Engineering Research Association, Auckland.
Kasai, K., Popov, E.P., 1986a. Cyclic Web Buckling Control for Shear Link Beams. J. Struct. Eng. 112, 505–523. https://doi.org/10.1061/(ASCE)0733-9445(1986)112:3(505)
Kasai, K., Popov, E.P., 1986b. A study of seismically resistant eccentrically braced frames (No. Report Number UCB/EERC-86/01). University of California, Berkeley, USA.
Kazemzadeh Azad, S., Topkaya, C., 2017. A review of research on steel eccentrically braced frames. J. Constr. Steel Res. 128, 53–73. https://doi.org/10.1016/j.jcsr.2016.07.032
Lasdon, L., Fox, R., Ratner, M., 1973. Nonlinear Optimization Using the Generalized Reduced Gradient Method. Rev. Fr. D'Automatique Inform. Rech. Opérationnelle Sér. Verte 8, 63. https://doi.org/10.1051/ro/197408V300731
Mansour, N., Christopoulos, C., Tremblay, R., 2011. Experimental Validation of Replaceable Shear Links for Eccentrically Braced Steel Frames. J. Struct. Eng. 137, 1141–1152. https://doi.org/10.1061/(ASCE)ST.1943-541X.0000350
McDaniel, C.C., Uang, C.-M., Seible, F., 2003. Cyclic Testing of Built-Up Steel Shear Links for the New Bay Bridge. J. Struct. Eng. 129, 801–809. https://doi.org/10.1061/(ASCE)0733-9445(2003)129:6(801)
Mulhall, D.G., Braungart, M., Hansen, K., 2019. Creating buildings with positive impacts.
NZS 3404 Part 1&2, 1997. Steel structures standard. Standards New Zealand, Wellington, New Zealand.
Okazaki, T., Engelhardt, M.D., 2007. Cyclic loading behavior of EBF links constructed of ASTM A992 steel. J. Constr. Steel Res. 63, 751–765.
Popov, E.P., Kasai, K., Engelhardt, M.D., 1987. Advances in design of eccentrically braced frames. Earthq. Spectra 3, 43–55.
Stratan, A., Dubina, D., 2004. Bolted links for eccentrically braced steel frames. Connect. Steel Struct. V 223–332.
Volynkin, D., Dusicka, P., Clifton, G.C., 2019. Intermediate Web Stiffener Spacing Evaluation for Shear Links. J. Struct. Eng. 145, 04018257. https://doi.org/10.1061/(ASCE)ST.1943-541X.0002244